

Pan-viral serology implicates enteroviruses in acute flaccid myelitis

Ryan D. Schubert^{1,2}, Isobel A. Hawes^{1,2,18}, Prashanth S. Ramachandran^{1,2,18}, Akshaya Ramesh^{1,2,18}, Emily D. Crawford^{3,4}, John E. Pak³, Wesley Wu³, Carly K. Cheung³, Brian D. O'Donovan⁵, Cristina M. Tato³, Amy Lyden³, Michelle Tan³, Rene Sit³, Gavin A. Sowa⁶, Hannah A. Sample⁵, Kelsey C. Zorn⁵, Debarko Banerji², Lillian M. Khan⁵, Riley Bove^{1,2}, Stephen L. Hauser^{1,2}, Amy A. Gelfand^{1,2}, Bethany L. Johnson-Kerner^{1,2}, Kendall Nash^{1,2}, Kalpathy S. Krishnamoorthy⁷, Tanuja Chitnis^{7,8}, Joy Z. Ding⁹, Hugh J. McMillan⁹, Charles Y. Chiu¹⁰, Benjamin Briggs¹¹, Carol A. Glaser¹², Cynthia Yen¹³, Victoria Chu¹³, Debra A. Wadford¹³, Samuel R. Dominguez¹⁴, Terry Fei Fan Ng¹⁵, Rachel L. Marine¹⁵, Adriana S. Lopez¹⁵, W. Allan Nix¹⁵, Ariane Soldatos¹⁶, Mark P. Gorman¹⁷, Leslie Benson¹⁷, Kevin Messacar¹⁴, Jennifer L. Konopka-Anstadt¹⁵, M. Steven Oberste¹⁵, Joseph L. DeRisi^{3,5} and Michael R. Wilson^{1,2*}

Since 2012, the United States of America has experienced a biennial spike in pediatric acute flaccid myelitis (AFM)¹⁻⁶. Epidemiologic evidence suggests non-polio enteroviruses (EVs) are a potential etiology, yet EV RNA is rarely detected in cerebrospinal fluid (CSF)². CSF from children with AFM ($n = 42$) and other pediatric neurologic disease controls ($n = 58$) were investigated for intrathecal antiviral antibodies, using a phage display library expressing 481,966 overlapping peptides derived from all known vertebrate and arboviruses (VirScan). Metagenomic next-generation sequencing (mNGS) of AFM CSF RNA ($n = 20$ cases) was also performed, both unbiased sequencing and with targeted enrichment for EVs. Using VirScan, the viral family significantly enriched by the CSF of AFM cases relative to controls was *Picornaviridae*, with the most enriched *Picornaviridae* peptides belonging to the genus *Enterovirus* ($n = 29/42$ cases versus $4/58$ controls). EV VP1 ELISA confirmed this finding ($n = 22/26$ cases versus $7/50$ controls). mNGS did not detect additional EV RNA. Despite rare detection of EV RNA, pan-viral serology frequently identified high levels of CSF EV-specific antibodies in AFM compared with controls, providing further evidence for a causal role of non-polio EVs in AFM.

First detected in California in 2012, the USA has experienced seasonal, biennial increases in the incidence of AFM cases⁷. Since 2014, the Centers for Disease Control and Prevention have reported

over 500 confirmed cases^{1-4,8}. The nationwide surges in AFM in 2014, 2016 and 2018 have coincided temporally and geographically with outbreaks of EV-D68 and EV-A71 infections^{2,6,9-11}. EVs, including poliovirus, are well recognized for their neuroinvasive capacity and resultant central nervous system (CNS) pathology, ranging from self-resolving aseptic meningitis to fulminant, sometimes fatal, brainstem encephalitis, and to myelitis leading to permanent debilitating paralysis¹².

Despite the temporal association between EV-D68 and EV-A71 outbreaks and AFM, and a mouse model that recapitulates the AFM phenotype with a contemporary EV-D68 strain¹³, the etiology of AFM has been difficult to confirm^{14,15}. Thus, concerns persist that AFM could result from yet-to-be-identified pathogens or a parainfectious immune response. This is due, in part, to the fact that less than half of the children with AFM have had EV detected in a non-sterile biologic specimen (nasopharyngeal or oropharyngeal swabs most commonly, rectal and stool samples less commonly), and no other alternative candidate etiologic agents have been identified in the remaining children³. In addition, only 2% of children with AFM have had EV nucleic acid detected in their CSF^{16,17}.

The immune-privileged status of the CNS makes direct detection of viral nucleic acid or indirect discovery of intrathecal antiviral antibodies an important step in linking a pathogen to a neuroinfectious disease. CSF was examined from AFM patients of recent outbreaks with unbiased ultra-deep mNGS, including with a novel

¹Weill Institute for Neurosciences, University of California, San Francisco, San Francisco, CA, USA. ²Department of Neurology, University of California, San Francisco, San Francisco, CA, USA. ³Chan Zuckerberg Biohub, San Francisco, CA, USA. ⁴Department of Microbiology and Immunology, University of California, San Francisco, San Francisco, CA, USA. ⁵Department of Biochemistry and Biophysics, University of California, San Francisco, San Francisco, CA, USA. ⁶School of Medicine, University of California, San Francisco, San Francisco, CA, USA. ⁷Department of Neurology, Massachusetts General Hospital, Boston, MA, USA. ⁸Department of Neurology, Brigham and Women's Hospital, Boston, MA, USA. ⁹Division of Neurology, Children's Hospital of Eastern Ontario, University of Ottawa, Ottawa, ON, Canada. ¹⁰Department of Laboratory Medicine and Medicine, Division of Infectious Diseases, University of California, San Francisco, San Francisco, CA, USA. ¹¹Department of Pediatrics, Division of Infectious Diseases, University of California, San Francisco, San Francisco, CA, USA. ¹²Department of Pediatric Infectious Diseases, Kaiser Permanente Oakland Medical Center, Oakland, CA, USA. ¹³Division of Communicable Disease Control, California Department of Public Health, Richmond, CA, USA. ¹⁴Children's Hospital Colorado and Department of Pediatrics, University of Colorado School of Medicine, Aurora, CO, USA. ¹⁵Division of Viral Diseases, Centers for Disease Control and Prevention, Atlanta, GA, USA. ¹⁶National Institute of Neurological Disorders and Stroke, National Institutes of Health, Bethesda, MD, USA. ¹⁷Department of Neurology, Boston Children's Hospital, Boston, MA, USA. ¹⁸These authors contributed equally: Isobel A. Hawes, Prashanth S. Ramachandran, Akshaya Ramesh. *e-mail: michael.wilson@ucsf.edu

Table 1 | Characteristics of the patients at baseline

	AFM cases	OND controls
<i>n</i>	42	58
Age—median (IQR), months	38 (11–64)	120 (66–174)
Sex—no. (%)		
Female	13 (31)	32 (55)
Male	29 (69)	26 (45)
Region—no. (%)		
USA		
West	20 (48)	37 (64)
South	7 (17)	4 (7)
Midwest	3 (7)	4 (7)
Northeast	11 (26)	9 (16)
International		
South America	0 (0)	2 (3)
Canada	1 (2)	0 (0)
North Atlantic Island	0 (0)	1 (2)
Middle East	0 (0)	1 (2)
Year—no. (%)		
2014	5 (12)	10 (17)
2015	0 (0)	14 (24)
2016	2 (5)	12 (21)
2017	0 (0)	8 (14)
2018	34 (81)	14 (24)
Season—no. (%)		
Spring	1 (2)	18 (31)
Summer	12 (29)	8 (14)
Fall	24 (57)	20 (34)
Winter	5 (12)	12 (21)
Suspected etiology—no. (%)		
Infectious	–	23 (40)
Autoimmune	–	22 (38)
Non-inflammatory	–	6 (10)
Malignancy	–	3 (5)
Unavailable	–	4 (7)

Percentages may not total 100 because of rounding.

CRISPR-Cas9-based enrichment technique called FLASH (finding low abundance sequences by hybridization)¹⁸. Furthermore, to search for virome-wide antibody signals that might be associated with AFM, the VirScan approach was used that had previously been developed to detect antibodies to all known human viruses¹⁹. To improve on this detection method, a larger and more finely tiled peptide library was generated in the T7 bacteriophage display vector as described in detail in Methods.

Results

Cases and controls. AFM cases, 42, and other neurologic disease (OND) controls, 58, were included in the present study (see Extended Data Fig. 1). Patient demographics are described in Table 1 with detailed information on available clinical diagnostic testing in Supplementary Tables 1A and 1B. The AFM cases were younger (median age 37.8 months, interquartile range (IQR), 11–64 months) than the OND controls (median age 120 months,

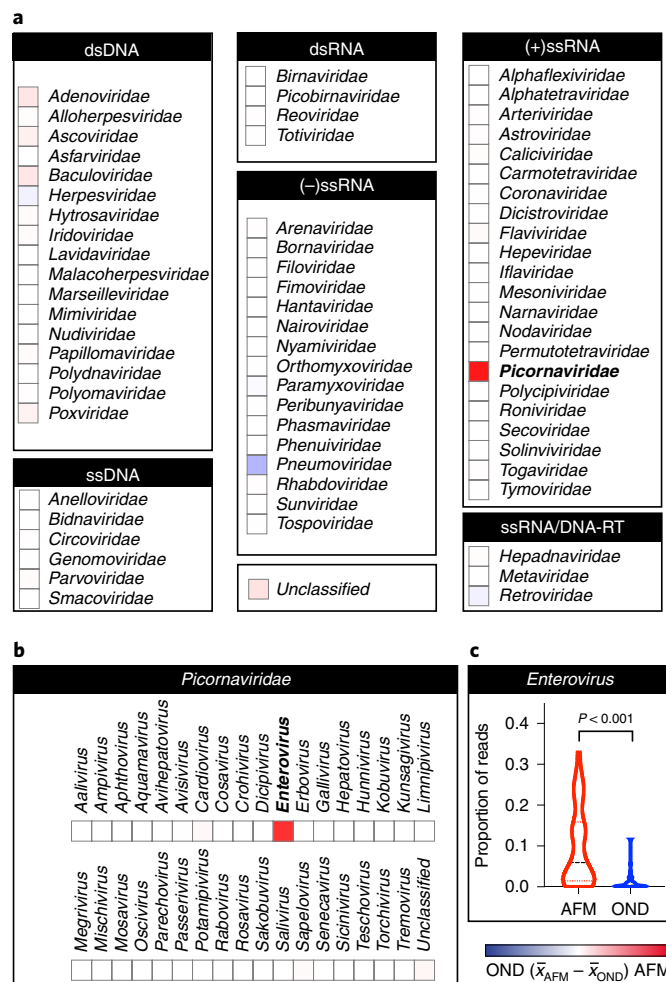


Fig. 1 | EV immunoreactivity in AFM on a pan-viral phage display assay. **a**, Viral families detected by VirScan or phage immunoprecipitation sequencing (PhIP-seq) sorted by their Baltimore classification. Heatmap color intensity was calculated by subtracting the mean rpK in the OND CSF sample set (*n* = 58) from that observed in AFM CSF (*n* = 42). The maximum and minimum color intensities reflect +11,000 and –11,000 rpK, respectively. The strongest intensity is observed in the *Picornaviridae* family (boldface type). DNA-RT, DNA reverse transcriptase; dsDNA, double-stranded DNA; dsRNA, double-stranded RNA; ssRNA, single-stranded RNA. **b**, Genus *Enterovirus* (boldface type) demonstrating the strongest enrichment in family *Picornaviridae*. **c**, Violin plot of the proportion of *Enterovirus* phage per patient with mean and first and third quartiles indicated by horizontal lines; Mann-Whitney test corrected for multiple comparisons with Bonferroni's adjustment.

IQR, 66–174 months), with a *P* value of 0.0497 (as determined by an unpaired parametric *t*-test). There was a higher proportion of males in the AFM cases. AFM cases and OND controls from the western and northeastern USA made up most of both categories. Most AFM cases were from 2018.

Ultra-deep mNGS rarely detects EV in AFM. An average of 433 million, 150-nucleotide (nt), paired-end reads per sample (range 304–569 million reads per sample) were obtained. Based on the External RNA Controls Consortium (ERCC) RNA spike-ins, it was estimated that our mean limit of detection was 5.48 attograms (range, 3.92–17.47 attograms)²⁰. EV-A71 was detected in one AFM sample at 71.31 reads per million sequences (rpM) (1,497.3 rpM in FLASH-NGS; see Supplementary Tables 2 and 3). This sample was

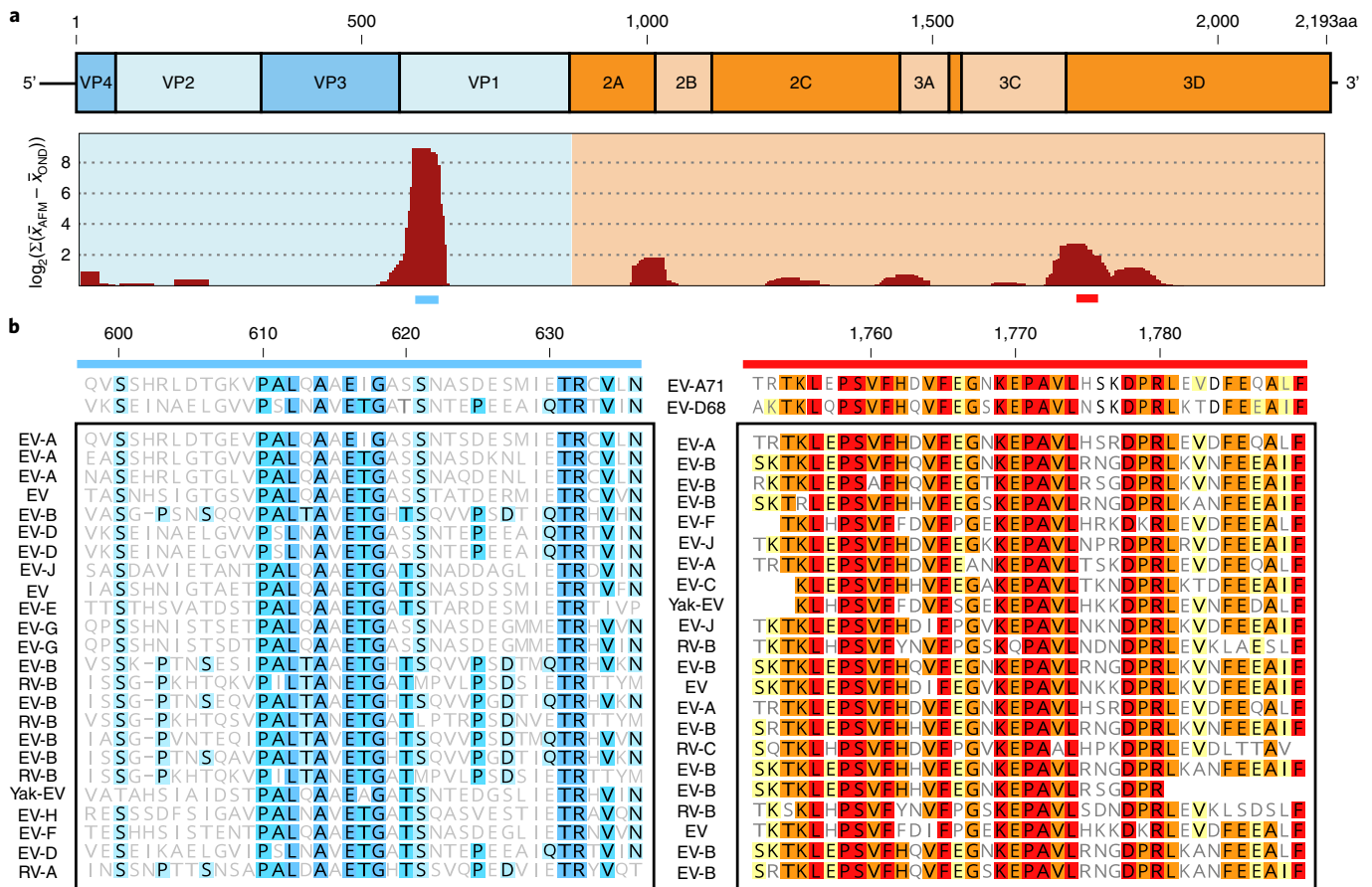


Fig. 2 | Primary EV antigens identified by pan-viral phage display in AFM. Some 438 unique, enriched antigens were identified with taxonomic identifications mapping to EV across all AFM CSF samples ($n=42$). **a**, EV-derived peptides (420 of 438) were mapped by BLASTP to the 2,193 amino acid (aa) polyprotein of EV-A71 (Genbank Accession [AXK59213.1](#)) as a model reference. The relative recovery of these peptides by VirScan is plotted as \log_2 of the sum of the differences in the mean signal generated in the AFM and pediatric OND cohorts, using a moving average of 32 amino acids, advanced by steps of 4 amino acids. **b**, Multiple sequence alignment of a representative set of enriched EV-derived peptides for the VP1 (blue bar) and 3D (red bar) proteins. Sequences from EV-D68 (Genbank Accession [A1T52326.1](#)) and EV-A71 (Genbank Accession [AXK59213.1](#)) are included for reference. Amino acids are shaded to indicate shared identity among peptides from the indicated EV species.

previously known to be EV-A71 positive by EV real-time PCR and Sanger sequencing. No other pathogenic organisms were detected in this or any of the other AFM samples. The non-human sequence reads from each sample were deposited at the National Center for Biotechnology Information Sequence Read Archive ([PRJNA557094](#)).

CSF VirScan detects EV antibodies in AFM. The only significantly enriched viral family by VirScan of CSF in AFM cases ($n=42$) versus OND controls ($n=58$) was *Picornaviridae* (mean reads per hundred thousand sequences (rpK) 11,082, IQR 16,850 versus mean rpK 1,121, IQR 974, P -adjusted value = 6.3×10^{-8} using the Mann-Whitney test with Bonferroni's adjustment; see Supplementary Table 4). Enriched *Picornaviridae* peptides belonged almost entirely to the genus *Enterovirus* (Fig. 1a–c, and see Supplementary Table 5), with 69% (29/42) of AFM cases versus 7% (4/58) of OND controls considered positive for EV antibodies by VirScan. Enriched EV peptides were derived from proteins across the EV genome (Fig. 2a, and see Supplementary Table 6A). Peptides mapping to *Sapelovirus* and unclassified *Picornaviridae* were also significantly enriched in AFM relative to OND controls (P -adjusted value = 0.013 and 0.00038, respectively using the Mann-Whitney test with Bonferroni's adjustment). Using the EV-A71 genome as a model reference EV, as in Fig. 2a, 99% and 95% of the rpK signal for *Sapelovirus* and unclassified *Picornaviridae*

mapped to EV-A71 using BLASTP (e-value threshold 0.01, word size 2) (see Supplementary Tables 6B and 6C).

Among capsid protein sequences, KVPALQAAEIGA in viral protein 1 (VP1) was previously reported to be an immunodominant linear EV epitope^{21,22}. Peptides containing this and related overlapping epitopes were enriched in the data across AFM patients, with multiple sequence alignment revealing a consensus motif of PXLAXEXG (Fig. 2b). Another immunodominant epitope was to a conserved, linear portion of 3D (Fig. 2c).

EV VP1 ELISA confirms VirScan findings. Consistent with the VirScan data, the mean EV VP1 ELISA signal in AFM ($n=26$, mean optical density (OD) 0.51, IQR 0.56) was significantly higher than OND controls ($n=50$, mean OD 0.08, IQR 0.06, $P < 0.001$ using the Mann-Whitney test; see Fig. 3 and per-patient data in Supplementary Tables 1A and 1B). The EV signal detected by phage and ELISA demonstrated a linear correlation ($R^2 = 0.511$, $P < 0.001$, see Extended Data Fig. 2). Among AFM patients, mean CSF EV antibody levels detected by either ELISA or VirScan did not differ based on whether EV RNA had been previously detected ($n=15$) or not ($n=11$) (mean OD 0.41 versus 0.65 by ELISA; mean rpK 6,093 versus 14,489 by VirScan, $P =$ not significant for both comparisons). In total, 85% (22/26) of a subset of AFM versus 14% (7/50) of OND tested by ELISA demonstrated reactivity against VP1. ELISA

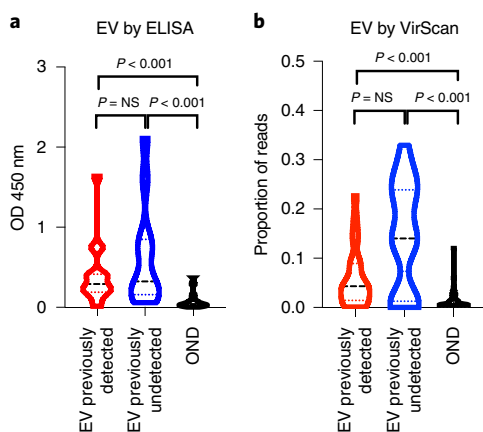


Fig. 3 | Independent validation of pan-viral phage display with purified EV VP1 capsid protein. **a**, Violin plot that EV signal generated by ELISA can be found at similar levels in AFM patients with previously detected ($n=15$) and previously undetected ($n=11$) EV infections ($P=NS$, not significant). In both AFM cohorts, there was a significantly greater amount of signal generated by ELISA compared with pediatric OND controls ($n=50$; $P < 0.001$ for both comparisons, Mann-Whitney test). **b**, Similar results by VirScan with no differences seen when comparing EV signal in AFM patients with previously detected ($n=23$) and previously undetected ($n=19$) EV infections ($P=NS$). When each group was compared with the OND controls ($n=58$), both demonstrated notable enrichment of EV signal ($P < 0.001$; Mann-Whitney test with Bonferroni's adjustment for multiple comparisons).

confirmed 18/19 EV-positive VirScan samples and identified 11 additional EV-positive samples. The additional samples detected by ELISA did have EV phage signal by VirScan, but were below the conservative threshold used for designating a sample as positive (see Supplementary Tables 1A and 1B).

No obvious independent effect of geography, year or season was observed on either the VirScan total EV enrichment or the ELISA VP1 EV data (see Extended Data Figs. 3–5). To the extent that the magnitude of CSF pleocytosis is a surrogate for the degree of inflammation and associated blood–brain barrier compromise, no correlation was found between the CSF cell count and the magnitude of EV antibodies as measured by either VirScan or VP1 ELISA (see Extended Data Fig. 6A). Furthermore, no relationship was found between the total CSF immunoglobulin G concentration and the results of EV antibody testing by either VirScan or ELISA (see Extended Data Fig. 6B). In addition, no difference was observed in the total CSF immunoglobulin G concentration between the subset of the AFM cases and OND controls for whom clinical laboratory data were available (see Extended Data Fig. 6C). Nor was a relationship observed between the input VirScan library and the immunoprecipitation results (see Extended Data Fig. 7).

An attempt was made to identify serologic signatures specific to EV-A71 or EV-D68 using both VirScan and VP1 ELISA, but both assays yielded cross-reactivity in patients with known EV infections due to either EV-A71 or EV-D68 (see Extended Data Fig. 8). Indeed, CSF from AFM cases was commonly enriched for antibodies targeting more than one EV species (see Extended Data Fig. 9, and see Supplementary Tables 1A and 1B).

Discussion

Unbiased ultra-deep mNGS was combined with an adaptation of the VirScan method for comprehensively detecting antiviral antibodies to investigate CSF from a relatively large ($n=42$) and geographically diverse subset of children presenting with AFM since 2014. Ultra-deep mNGS, combined with FLASH enrichment for EV-A71 and

EV-D68, confirmed the presence of EV RNA in a single sample that was previously known to be positive for EV-A71 by PCR, but failed to discover any other pathogen in this or other AFM CSF samples. There are a number of possible reasons for the lack of detectable EV nucleic acid in the CSF of AFM patients when using mNGS or other methods. Clinically, radiologically and similarly to poliomyelitis, the CNS tissue involved in AFM is often restricted to the anterior horn cells in the cervical spinal cord, making it possible that little to no virus is shed into the CSF. In addition, children with AFM, especially when associated with EV-D68, typically present with neurologic symptoms a median of 5–7 d after prodromal illness onset, decreasing the probability of RNA detection²³.

Lack of consistent identification of viral nucleic acid in CSF is not limited to AFM; rather it is common to a wide range of neuroinvasive viruses, including poliovirus, rabies virus, West Nile virus and other arboviruses²⁴. As a result, detection of intrathecal antibody production through CSF serologic testing is the gold standard for diagnosis of many neuroinvasive viruses, notably West Nile virus and varicella-zoster virus^{25,26}. Thus, CSF mNGS was supplemented with VirScan to comprehensively profile CSF antiviral antibodies in AFM cases and OND controls¹⁹. VirScan revealed high levels of CSF immunoreactivity to immunodominant EV epitopes in AFM, independent of whether EV RNA had previously been detected in clinical testing of CSF or nonsterile sites. There was a non-significant trend toward greater enrichment of EV antibodies in patients without directly detectable virus in a peripheral site, however, possibly owing to the rise in titer that occurs in the weeks after an infection. Independent testing with EV-A71 and EV-D68 VP1 ELISAs confirmed this trend. VirScan and whole VP1 ELISA could not consistently identify specific individual EV types, probably owing to cross-reactive immune responses to conserved linear EV antigens²⁷. Future studies using well-folded virus, rather than linear phage display peptides or individual viral proteins, may be more fruitful for identifying a species-specific serologic signature.

The present study has important limitations. First, detection of a serologic response to a virus at a single time point, by itself, does not fulfill Koch's postulates for establishing causality between a virus and a particular disease. None the less, these serologic data support the specificity of the CSF antibody response to EVs in AFM, helping to fulfill the Bradford Hill criteria for making a causal association^{14,15}. Second, further work will be necessary to establish, in a prospective manner, the diagnostic sensitivity and specificity for CSF EV serology. Third, the cases and controls of the present study were not optimally matched. Although the controls had a diversity of pediatric ONDs, the case and control cohorts were not similar by age, year or season, which are important risk factors for EV infection in the USA. However, a notable effect of year or season was not seen on EV signal by VirScan or ELISA in the OND controls. It was decided to report these preliminary findings, despite the limitations of the study design, because of the public health urgency of understanding the etiology of AFM. A prospective study with matched cases and controls is necessary to confirm the findings.

AFM is a potentially devastating neurologic syndrome with the incidence of reported cases having risen in the USA since 2014 with biennial peaks. In addition, cases have now been detected in 14 other countries across 6 continents²³. There are no proven treatments for AFM and, similar to poliomyelitis, a vaccine may ultimately be the most effective prevention strategy. However, it is important to first achieve consensus around the probable etiologic agents. Although continued vigilance for other possible etiologies of AFM is warranted, together the combined mNGS, VirScan and viral protein ELISA investigation of AFM CSF supports the notion that EV infection probably underlies most AFM cases tested in the present study. These results offer a roadmap for rapid development of EV CSF antibody assays to enable efficient clinical diagnosis of EV-associated AFM in the future.

Online content

Any methods, additional references, Nature Research reporting summaries, source data, statements of code and data availability and associated accession codes are available at <https://doi.org/10.1038/s41591-019-0613-1>.

Received: 8 July 2019; Accepted: 13 September 2019;
Published online: 21 October 2019

References

- Sejvar, J. J. et al. Acute flaccid myelitis in the United States, August–December 2014: results of nationwide surveillance. *Clin. Infect. Dis.* **63**, 737–745 (2016).
- Van Haren, K. et al. Acute flaccid myelitis of unknown etiology in California, 2012–2015. *JAMA* **314**, 2663–2671 (2015).
- Greninger, A. L. et al. A novel outbreak enterovirus D68 strain associated with acute flaccid myelitis cases in the USA (2012–14): a retrospective cohort study. *Lancet Infect. Dis.* **15**, 671–682 (2015).
- McKay, S. L. et al. Increase in acute flaccid myelitis—United States, 2018. *MMWR Morb. Mortal. Wkly Rep.* **67**, 1273–1275 (2018).
- Centers for Disease Control and Prevention. AFM Confirmed U.S. Cases to Date. <https://www.cdc.gov/acute-flaccid-myelitis/afm-investigation.html> (accessed 3 October 2019).
- Messacar, K., Pretty, K., Reno, S. & Dominguez, S. R. Continued biennial circulation of enterovirus D68 in Colorado. *J. Clin. Virol.* **113**, 24–26 (2019).
- Ayscue, P. et al. Acute flaccid paralysis with anterior myelitis - California, June 2012–June 2014. *MMWR Morb. Mortal. Wkly Rep.* **63**, 903–906 (2014).
- Pruss, H. et al. N-Methyl-D-aspartate receptor antibodies in herpes simplex encephalitis. *Ann. Neurol.* **72**, 902–911 (2012).
- Aliabadi, N. et al. Enterovirus D68 infection in children with acute flaccid myelitis, Colorado, USA, 2014. *Emerg. Infect. Dis.* **22**, 1387–1394 (2016).
- Iverson, S. A. et al. Notes from the field: cluster of acute flaccid myelitis in five pediatric patients—Maricopa County, Arizona, 2016. *MMWR Morb. Mortal. Wkly Rep.* **66**, 758–760 (2017).
- Messacar, K. et al. Notes from the field: enterovirus A71 neurologic disease in children—Colorado, 2018. *MMWR Morb. Mortal. Wkly Rep.* **67**, 1017–1018 (2018).
- Jubelt, B. & Lipton, H. L. Enterovirus/picornavirus infections. *Handb. Clin. Neurol.* **123**, 379–416 (2014).
- Hixon, A. M. et al. A mouse model of paralytic myelitis caused by enterovirus D68. *PLoS Pathog.* **13**, e1006199 (2017).
- Dyda, A., Stelzer-Braid, S., Adam, D., Chughtai, A. A. & MacIntyre, C. R. The association between acute flaccid myelitis (AFM) and Enterovirus D68 (EV-D68)—what is the evidence for causation? *Euro. Surveill.* **23**, 17-00310 (2018).
- Messacar, K. et al. Enterovirus D68 and acute flaccid myelitis—evaluating the evidence for causality. *Lancet Infect. Dis.* **18**, e239–e247 (2018).
- Messacar, K. et al. Acute flaccid myelitis: a clinical review of US cases 2012–2015. *Ann. Neurol.* **80**, 326–338 (2016).
- Moline, H. et al. Notes from the field: six cases of acute flaccid myelitis in children—Minnesota, 2018. *MMWR Morb. Mortal. Wkly Rep.* **68**, 356–358 (2019).
- Quan, J. et al. FLASH: a next-generation CRISPR diagnostic for multiplexed detection of antimicrobial resistance sequences. *Nucleic Acids Res.* **47**, e83 (2019).
- Xu, G. J. et al. Viral immunology. Comprehensive serological profiling of human populations using a synthetic human virome. *Science* **348**, aaa0698 (2015).
- Baker, S. C. et al. The external RNA controls consortium: a progress report. *Nat. Meth.* **2**, 731–734 (2005).
- Gao, F. et al. Enterovirus 71 viral capsid protein linear epitopes: identification and characterization. *Virol. J.* **9**, 26 (2012).
- Mishra, N. et al. Antibodies to enteroviruses in cerebrospinal fluid of patients with acute flaccid myelitis. *MBio* **10**, e01903-19 (2019).
- Messacar, K. & Tyler, K. L. Enterovirus D68-associated acute flaccid myelitis: rising to the clinical and research challenges. *JAMA* **321**, 831–832 (2019).
- Ramachandran, P. S. & Wilson, M. R. Diagnostic testing of neurologic infections. *Neurol. Clinics* **36**, 687–703 (2018).
- Gilden, D., Cohrs, R. J., Mahalingam, R. & Nagel, M. A. Varicella zoster virus vasculopathies: diverse clinical manifestations, laboratory features, pathogenesis, and treatment. *Lancet Neurol.* **8**, 731–740 (2009).
- Chabierski, S. et al. Distinguishing West Nile virus infection using a recombinant envelope protein with mutations in the conserved fusion-loop. *BMC Infect. Dis.* **14**, 246 (2014).
- Samuelson, A., Forsgren, M., Johansson, B., Wahren, B. & Sallberg, M. Molecular basis for serological cross-reactivity between enteroviruses. *Clin. Diagn. Lab. Immunol.* **1**, 336–341 (1994).

Acknowledgements

This work is supported by a National Multiple Sclerosis Society—American Brain Foundation Clinician Scientist Development Award (no. FAN-1608-25607 to R.D.S.), the UCSF Biomedical Sciences Graduate Program (to I.A.H.), an American Academy of Neurology Clinical Research Training Scholarship (no. P0534134 to P.S.R.), the University of California, San Francisco (UCSF) Dean's Office Medical Student Research Program (G.A.S.), UCSF Bioinformatics Graduate Program (B.O.), NIH grant nos. K08NS096117 (to M.R.W.) and K23AI28069 (to K.M.), the Chan Zuckerberg Biohub (J.L.D., C.M.T., J.E.P., E.D.C., W.W., C.K.C., A.L., M.T. and R.S.), an endowment from the Rachleff family (to M.R.W.), and the Sandler and William K. Bowes, Jr. Foundations (M.R.W., K.C.Z., H.A.S., C.Y.C., L.M.K., B.O. and J.L.D.). We thank H. Sandler, W. Bowes, Jr., and D. and A. Rachleff for their encouragement. We thank the patients and their families for their participation in this study.

Author contributions

A.R. computationally designed the VirScan peptide library. R.D.S., I.A.H. and G.A.S. cloned the VirScan library. R.D.S. and I.A.H. performed the VirScan experiments. R.D.S. and B.O. developed the automated IP protocols and analysis pipeline for VirScan. J.E.P., W.W. and C.K.C. cloned and expressed EV VP1 proteins. R.D.S. performed the ELISA experiments. P.S.R., E.D.C., A.L., C.M.T., M.T. and R.S. performed metagenomic sequencing and FLASH. P.S.R., M.R.W. and E.D.C. analyzed metagenomic and FLASH data. D.B. and L.M.K. helped prepare samples for sequencing. R.D.S., H.A.S., K.C.Z., R.B., S.L.H., A.A.G., B.L.J.-K., K.N., K.S.K., T.C., J.Z.D., H.J.M., C.Y.C., B.B., C.A.G., C.Y., V.C., D.A.W., S.R.D., R.L.M., A.S.L., W.A.N., A.S., M.P.G., L.B., K.M., J.L.K.-A. and M.S.O. identified patients, performed clinical phenotyping and provided patient samples. R.D.S., A.R., T.F.F.N., J.L.D. and M.R.W. analyzed VirScan and ELISA data. R.D.S. and J.L.D. generated the figures. J.L.K.-A. and M.S.O. provided critical expert guidance on the manuscript. R.D.S., J.L.D. and M.R.W. conceived of and wrote the manuscript. All authors discussed the results and contributed critical reviews to the manuscript.

Competing interests

The authors declare no competing interests.

Additional information

Supplementary information is available for this paper at <https://doi.org/10.1038/s41591-019-0613-1>.

Correspondence and requests for materials should be addressed to M.R.W.

Peer review information Alison Farrell and Saheli Sadanand are the primary editors on this article and managed its editorial process and peer review in collaboration with the rest of the editorial team.

Reprints and permissions information is available at www.nature.com/reprints.

Publisher's note Springer Nature remains neutral with regard to jurisdictional claims in published maps and institutional affiliations.

Disclaimer The findings and conclusions in this report are those of the author(s) and do not necessarily represent the official position of the Centers for Disease Control and Prevention, the National Institutes of Health or the California Department of Public Health.

This is a U.S. government work and not under copyright protection in the U.S.; foreign copyright protection may apply 2019

Methods

Detailed methods for data collection, human subject review, mNGS, VirScan, bioinformatics and independent confirmatory testing with ELISA are provided in the Supplementary Appendix.

Case–control design. All AFM cases met the 2018 US Council of State and Territorial Epidemiologists' case definition for probable or confirmed AFM (see Supplementary Table 7)²⁸. Patient samples were collected with informed consent either through enrollment in research studies or through public health surveillance. In addition, residual banked CSF was obtained from children with ONDs without suspected primary EV infection and without known exposure to intravenous gamma-globulin for controls.

Metagenomic sequencing library preparation. CSF was shipped on dry ice to the laboratory and stored immediately on receipt at -80°C until use. RNA-sequencing libraries were prepared using a previously described protocol optimized and adapted for miniaturization and automation²⁹. Libraries were sequenced on a NovaSeq 6000 machine (Illumina) to generate 150-nt, paired-end reads. Samples were also sequenced after enrichment for EV-A71 and EV-D68 genomes using FLASH (see Supplementary Table 2)¹⁸. All NGS libraries were depleted of host ribosomal RNA with DASH (depletion of abundant sequences by hybridization) and spiked-in with ERCC sequences as previously described^{20,30}.

Metagenomic bioinformatics. As previously described, pathogens were identified from raw mNGS sequencing reads using IDseq v.3.2, a cloud-based, open-source bioinformatics platform designed for detection of microbes from mNGS data³¹.

Pan-viral CSF serologic testing with VirScan. The previously published VirScan method is an application of phage immunoprecipitation sequencing (PhIP-seq), displaying viral peptides on the outer surface of bacteriophages for the purposes of antibody detection, followed by deep sequencing^{29,32}. Similarly, a T7 bacteriophage display library was constructed, comprising 481,966 peptides of 62 amino acids with a 14-amino-acid overlap tiled across a representative set of full-length, vertebrate, mosquito-borne and tick-borne viral genomes downloaded from the UniProt and RefSeq databases in February 2017 (see Supplementary Table 8A–D). After amplification, phage libraries were incubated with 2 μl of patient CSF overnight and then immunoprecipitated for two rounds as previously described^{33,34}. Barcoded phage DNA was sequenced on a HiSeq 4000 machine (Illumina) using 150-nt, paired-end reads.

VirScan bioinformatics. Sequencing reads were aligned to a reference database comprising the full viral peptide library. Peptide counts were normalized by dividing by the sum of counts and multiplying by 100,000 (rpK)^{33–36}. Phage rpK results for each phage in each subject were filtered using a cutoff fold change of greater than 10 above the mean background rpK generated from null IPs (see Supplementary Table 9). A sample was considered EV positive if the total EV rpK value was greater than the mean signal in the OND controls plus 1 s.d.

Independent validation with ELISA. To independently validate the VirScan results, recombinant VP1 was generated from recent AFM-associated EV-A71

and EV-D68 strains and ELISA performed to detect EV antibodies with AFM CSF samples for which sufficient CSF remained ($n=26$) and OND controls ($n=50$). The signal was measured as the OD at 450 nm and reported after background subtraction (background OD = 0.05). For each sample, the higher of the two (EV-A71 or EV-D68) OD values was considered when analyzing cases and controls. A sample was considered positive if the reported OD was more than three times the background.

Statistical methods. VirScan data comparisons between AFM cases and OND controls were made using the Mann–Whitney test with Bonferroni's adjustment for multiple comparisons: $n=42$ AFM cases and $n=58$ OND controls. EV VP1 signal by ELISA was compared between $n=26$ AFM cases and $n=50$ OND controls using the Mann–Whitney test. When subsets were tested, exact n values and statistical tests are provided in the figure legends. All error bars are defined in the figure legends.

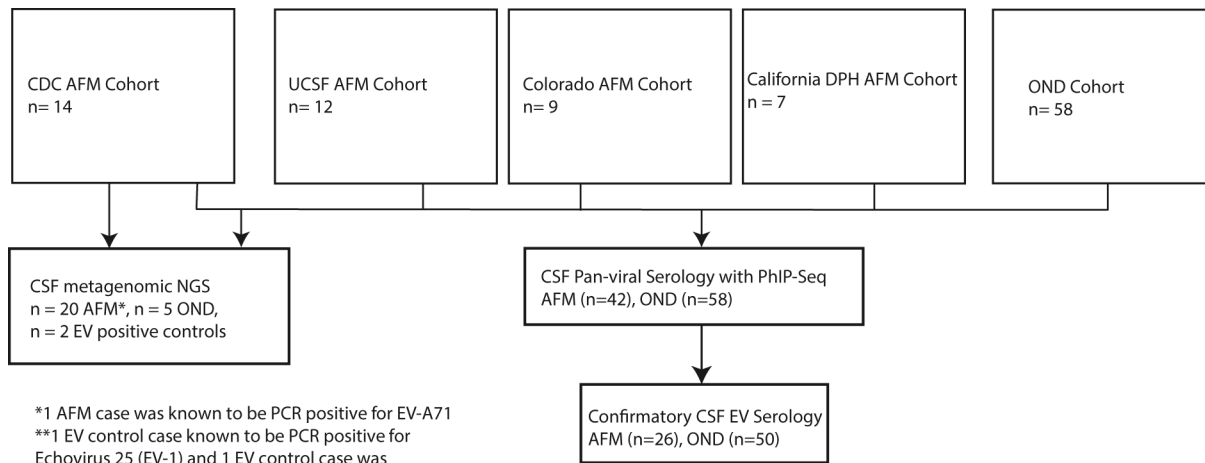
Reporting Summary. Further information on research design is available in the Nature Research Reporting Summary linked to this article.

Data availability

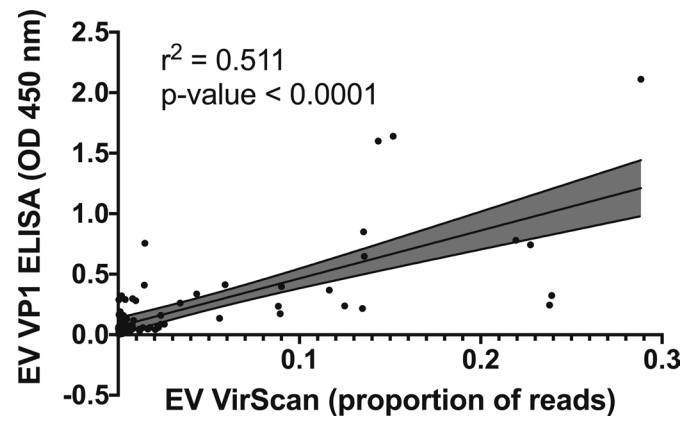
VirScan and clinical data analyzed in the manuscript have been made available in the online Supplementary material. The non-human sequence reads from the mNGS experiments for each sample were deposited at the National Center for Biotechnology Information Sequence Read Archive (PRJNA557094).

References

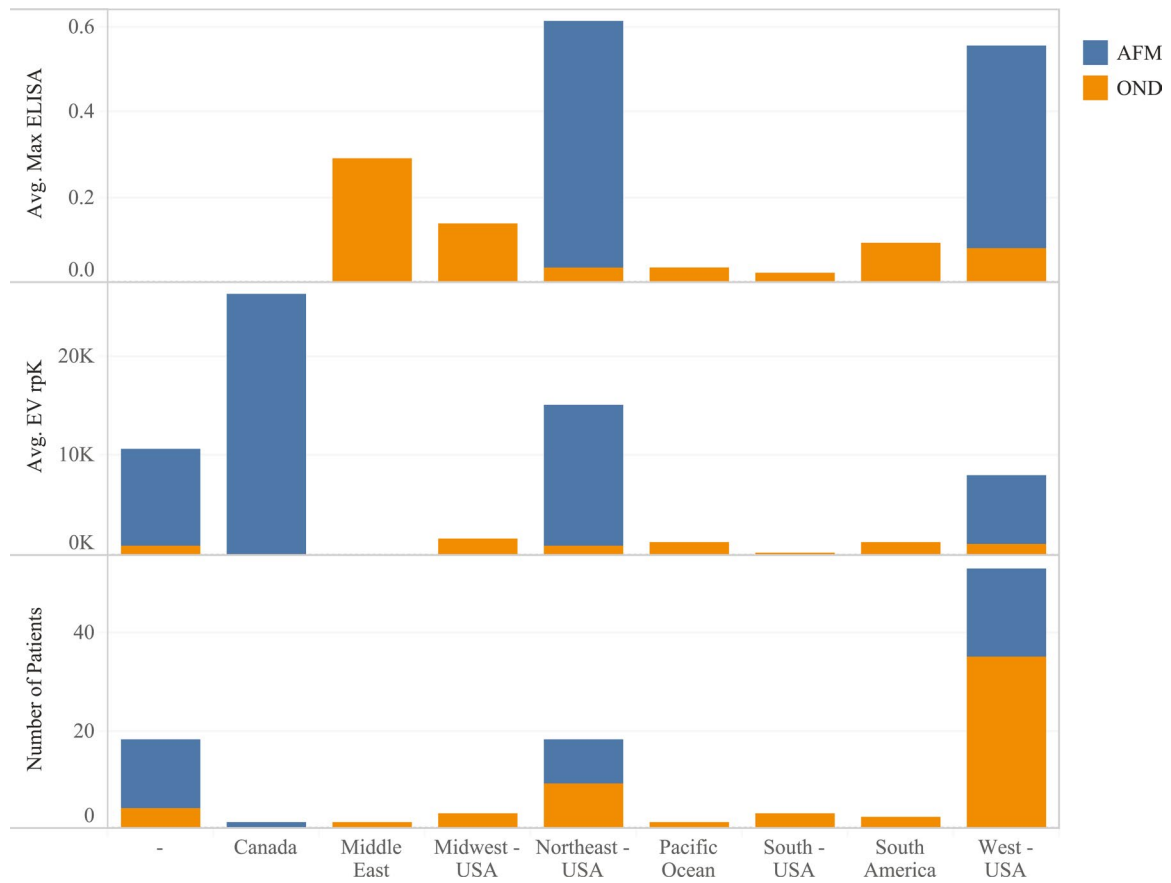
- Revision to the Standardized Surveillance and Case Definition for Acute Flaccid Myelitis (Council of State and Territorial Epidemiologists, 2018); <https://cdn.ymaws.com/www.cste.org/resource/resmgr/2017ps/2017psfinal/17-ID-01.pdf>
- Mayday, M. Y., Khan, L. M., Chow, E. D., Zinter, M. S. & DeRisi, J. L. Miniaturization and optimization of 384-well compatible RNA sequencing library preparation. *PLoS ONE* **14**, e0206194 (2019).
- Gu, W. et al. Depletion of abundant sequences by hybridization (DASH): using Cas9 to remove unwanted high-abundance species in sequencing libraries and molecular counting applications. *Genome Biol.* **17**, 41 (2016).
- Ramesh, A. et al. Metagenomic next-generation sequencing of samples from pediatric febrile illness in Tororo, Uganda. *PLoS ONE* **14**, e0218318 (2019).
- Pou, C. et al. The repertoire of maternal anti-viral antibodies in human newborns. *Nat. Med.* **25**, 591–596 (2019).
- O'Donovan, B. et al. Exploration of anti-Yo and anti-Hu paraneoplastic neurological disorders by PhIP-Seq reveals a highly restricted pattern of antibody epitopes. Preprint at *bioRxiv* <https://doi.org/10.1101/502187> (2018).
- Mandel-Brehm, C. et al. Kelch-like protein 11 antibodies in seminoma-associated paraneoplastic encephalitis. *N. Engl. J. Med.* **381**, 47–54 (2019).
- Zhang, J., Kobert, K., Flouri, T. & Stamatakis, A. PEAR: a fast and accurate Illumina paired-end reAd mergeR. *Bioinformatics* **30**, 614–620 (2014).
- Langmead, B. & Salzberg, S. L. Fast gapped-read alignment with Bowtie 2. *Nat. Meth.* **9**, 357–359 (2012).



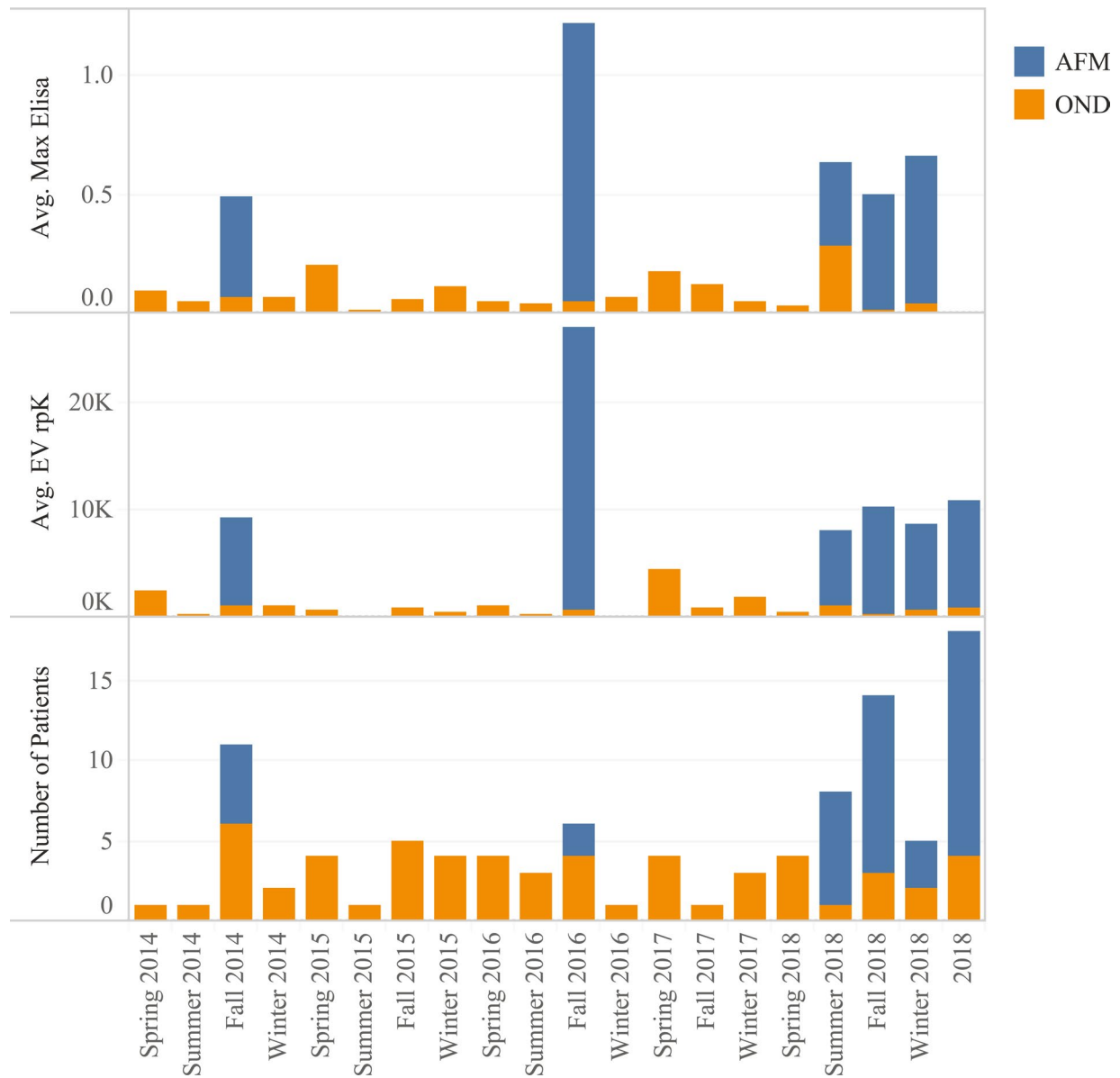
Extended Data Fig. 1 | Flow chart depicting patient enrollment by institution. mNGS with and without FLASH were performed on CSF samples acquired from the CDC (n=14 AFM, n=4 OND, n=2 EV positive controls) and UCSF AFM Cohort (n=6 AFM). Samples from all institutions were tested by VirScan. Due to limited sample, a subset of those tested by VirScan were tested by confirmatory ELISA.



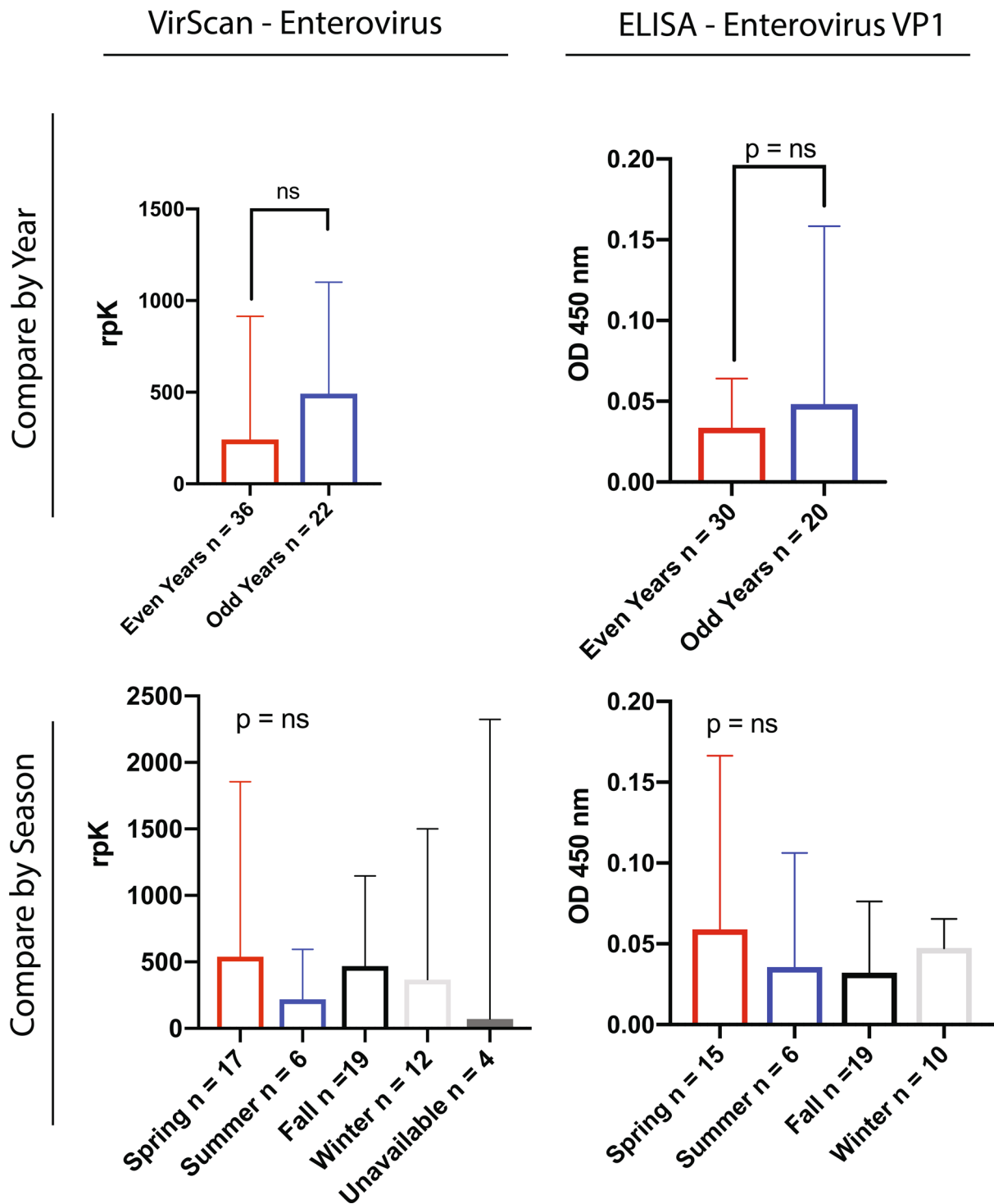
Extended Data Fig. 2 | Comparison of VirScan and ELISA. A comparison of the total amount of enterovirus signal generated by VirScan (x-axis) to the maximum OD generated by either EV-D68 or EV-A71 signal ELISA (greater of the two values shown) for all samples run ($n = 26$ AFM + 50 OND). The 95% confidence intervals are shaded in grey.



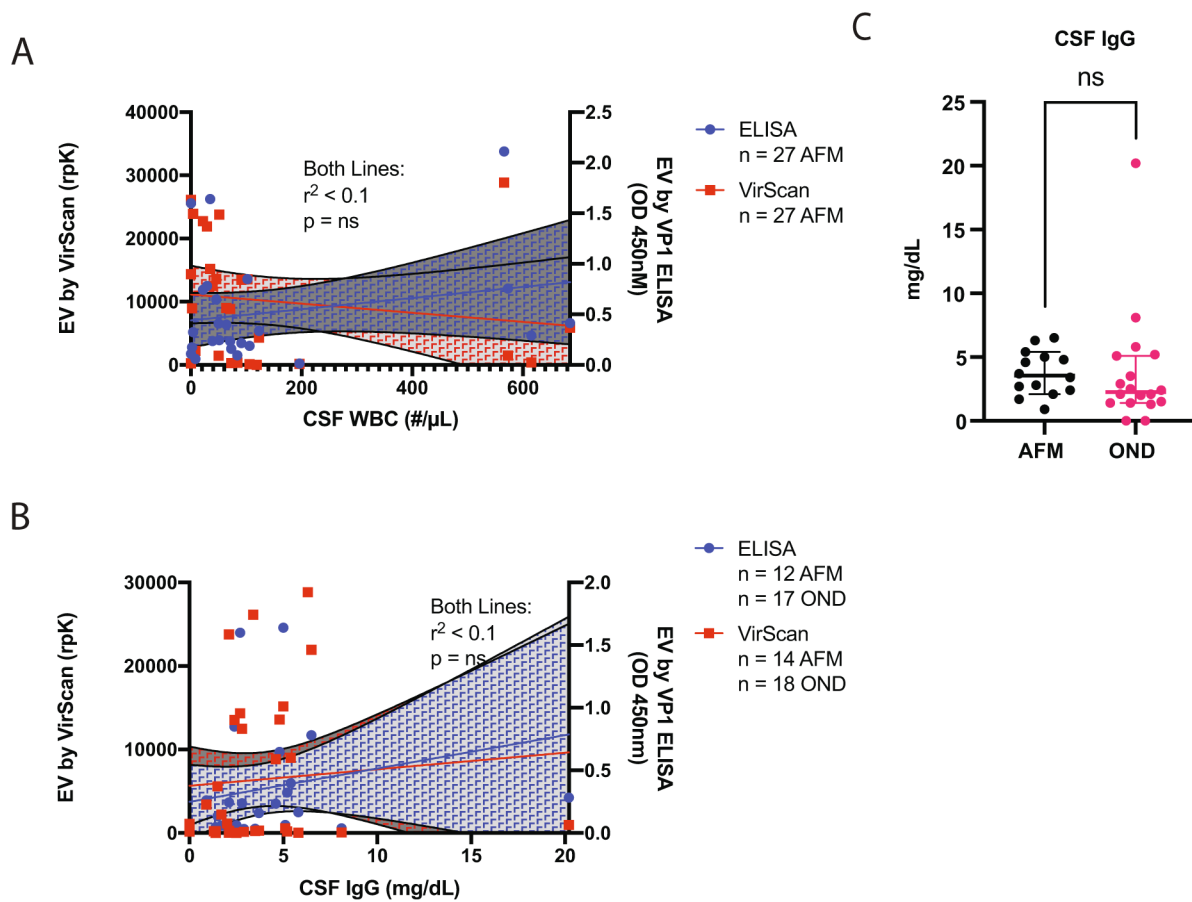
Extended Data Fig. 3 | Geographic distribution of cases and controls. Geographic comparison of cases (blue) and controls (orange) with average EV signal by ELISA (top), average EV signal by VirScan (middle), and total number (bottom).



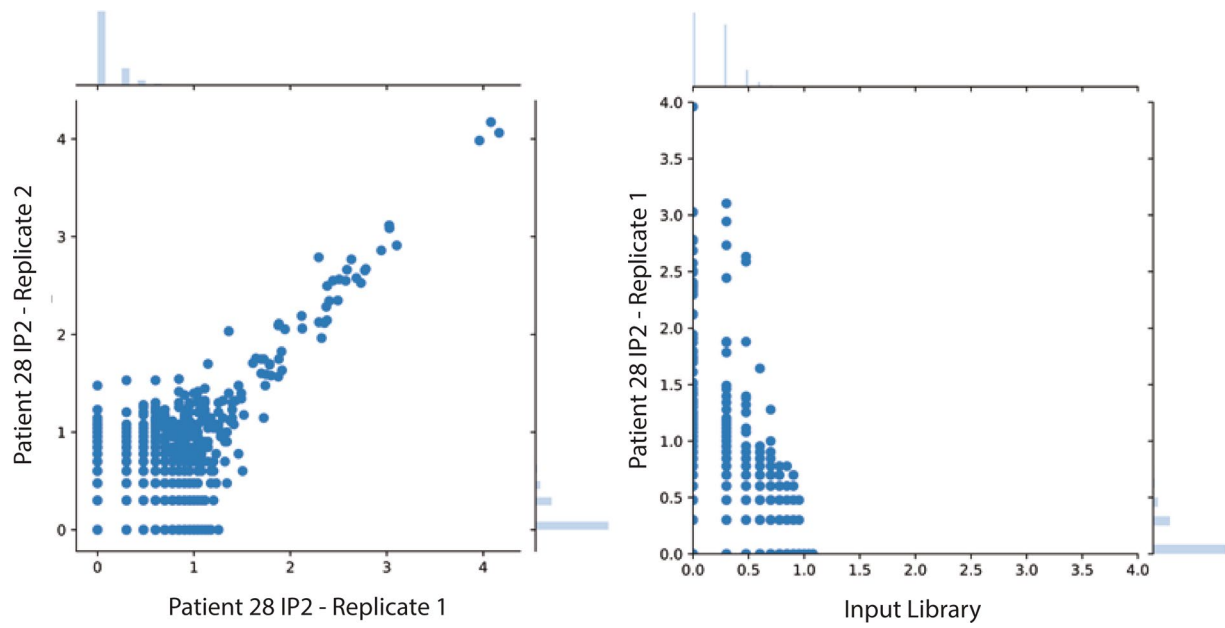
Extended Data Fig. 4 | Season and year of cases and controls. Season and year comparison for cases (blue) and controls (orange) with average EV signal by ELISA (top), average EV signal by VirScan (middle), and total number (bottom).



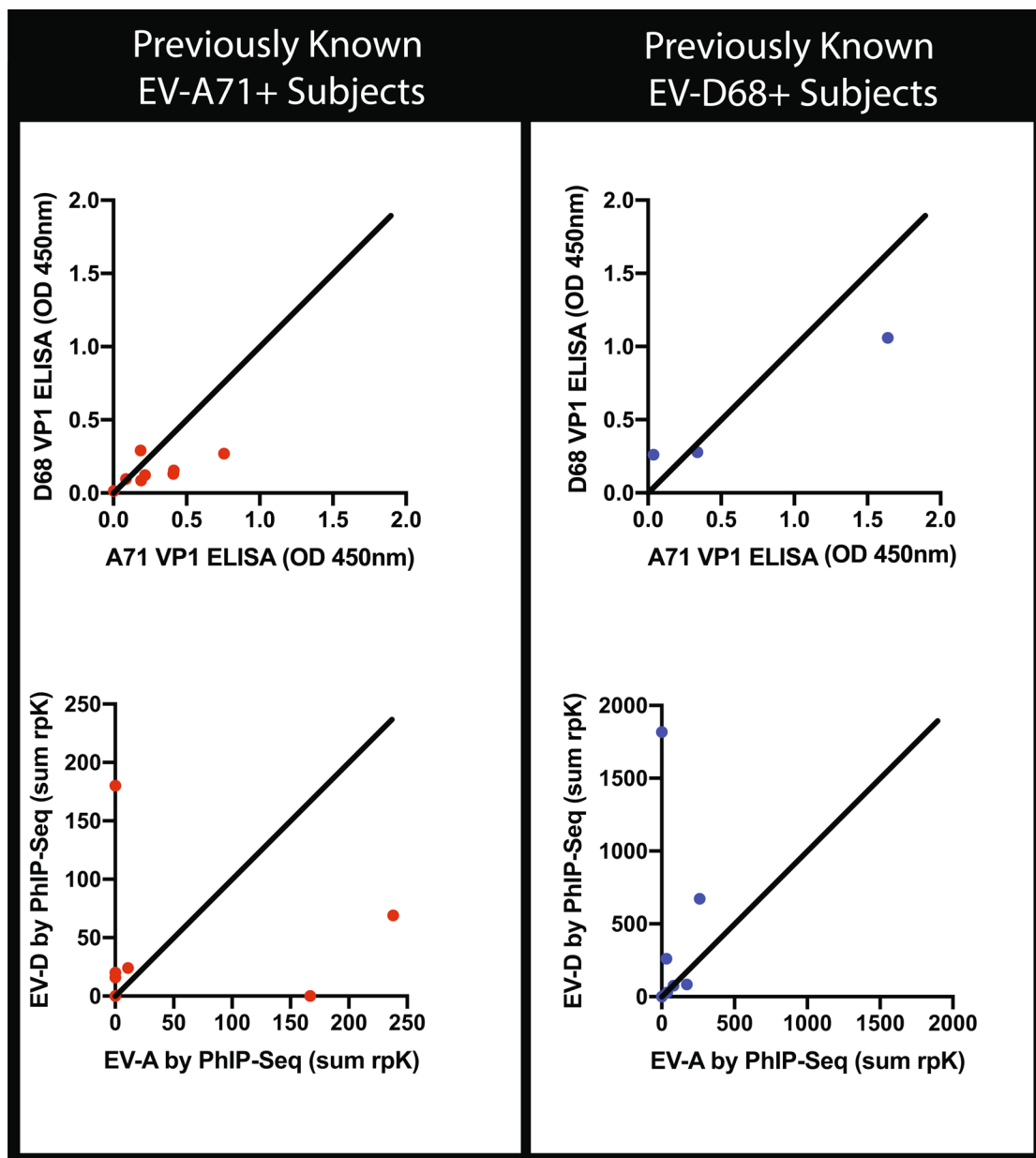
Extended Data Fig. 5 | Analysis of effect of year and season on enterovirus signal in the OND controls. EV VirScan (left, n = 54) and EV VP1 ELISA (right, n = 50) for the OND control cohort by year (top) and season (bottom). Bar graphs depict heights as median values with error bars reflecting the interquartile range. Statistics for year were performed with the Mann-Whitney test and for seasons with the Kruskal-Wallis test.



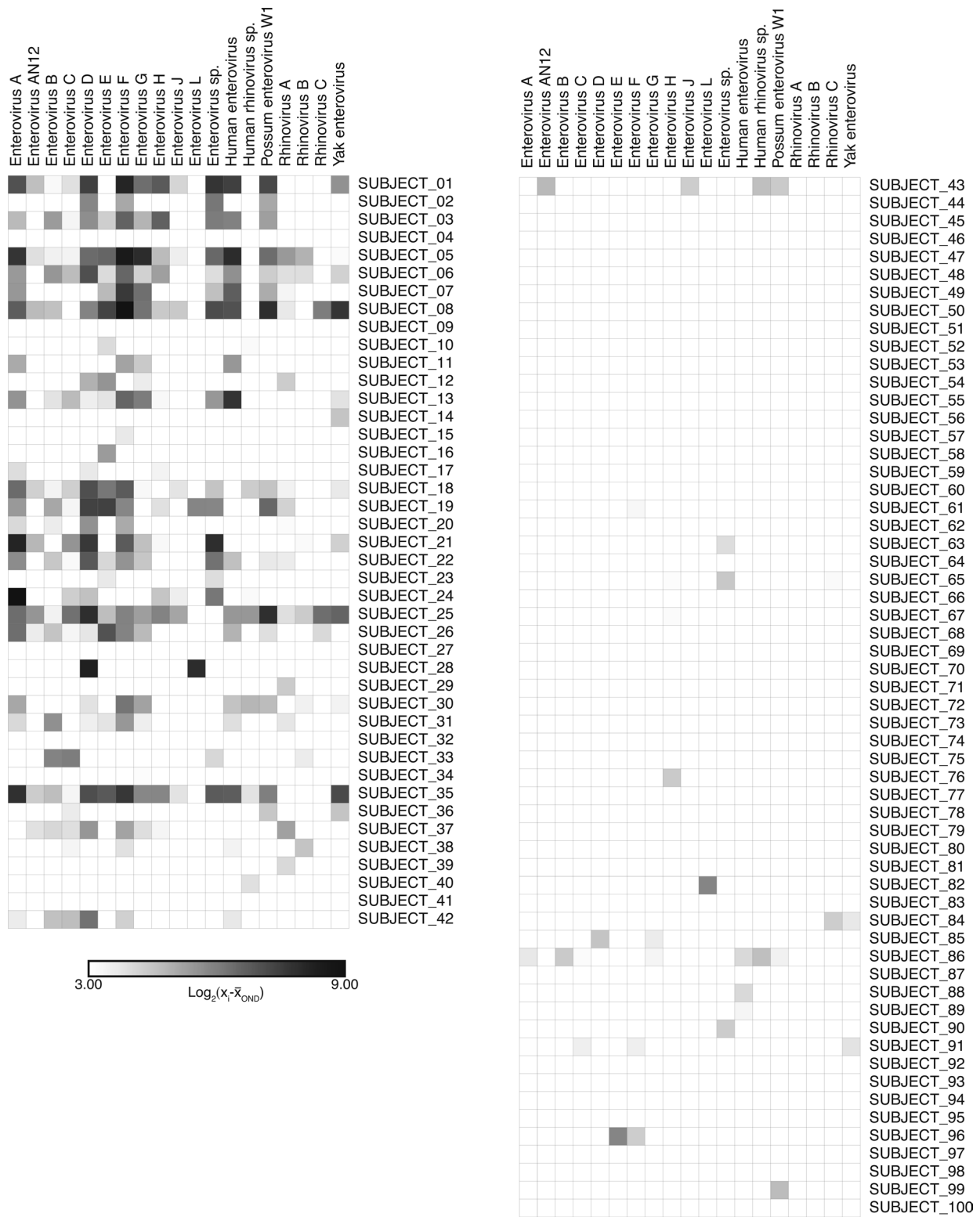
Extended Data Fig. 6 | CSF cell count and IgG concentration in cases and controls do not explain EV signal by VirScan or ELISA. CSF enterovirus antibodies by VirScan and ELISA are not correlated with the overall amount of CNS inflammation as measured by the CSF cell count (panel A) or CSF IgG (panel B) in a subset of patients. The 95% confidence intervals for each measurement are shaded in blue (ELISA) or red (VirScan). When comparing the concentration of IgG in a subset of AFM cases and OND controls, there was no difference in CSF IgG concentration ($p = ns$ by Mann-Whitney, mean with errors bars showing standard deviation displayed). Two OND CSF IgG values were reported as < 0.9 mg/dL and were conservatively estimated to be 0. Errors bars represent 95% confidence intervals.



Extended Data Fig. 7 | Enterovirus antibody enrichment in AFM cases with VirScan is not a reflection of bias in the input library. Dotplot demonstrating replicate IPs from a typical sample (left panel) correlate with each other but not with the input library (right panel). Values plotted are \log_{10} of the raw rpK values + 1. The sum of the signal at each point on the axes is expressed as a barplot on the axes of the graph.



Extended Data Fig. 8 | Strain calling by ELISA versus VirScan. ELISA and VirScan data from subjects with EV-A71 or EV-D68 detected by RT-PCR in either CSF, stool or respiratory fluid. Top panels with strain-specific VP1 ELISA data from EV-A71 ($n = 8$, red) and EV-D68 ($n = 3$, blue) patients show cross reactivity. Bottom panels show VirScan data from known EV-A71 ($n = 9$, red) and EV-D68 ($n = 7$, blue) patients. EV-A and EV-D signals were generated by summing the total rpK generated against EV-A and EV-D derived peptides within a sample.



Extended Data Fig. 9 | Enterovirus species per-subject heatmap. VirScan enterovirus signal in each subject demonstrating enrichment for a cross-reactive EV signal in the AFM subjects (left) as compared with OND subjects (right). Signal represents the \log_2 of the subject's EV rpK value divided by the mean rpK value in the OND subjects for each EV species. To increase clarity, values below 3 are not shown.

Reporting Summary

Nature Research wishes to improve the reproducibility of the work that we publish. This form provides structure for consistency and transparency in reporting. For further information on Nature Research policies, see [Authors & Referees](#) and the [Editorial Policy Checklist](#).

Statistics

For all statistical analyses, confirm that the following items are present in the figure legend, table legend, main text, or Methods section.

n/a Confirmed

- The exact sample size (n) for each experimental group/condition, given as a discrete number and unit of measurement
- A statement on whether measurements were taken from distinct samples or whether the same sample was measured repeatedly
- The statistical test(s) used AND whether they are one- or two-sided
Only common tests should be described solely by name; describe more complex techniques in the Methods section.
- A description of all covariates tested
- A description of any assumptions or corrections, such as tests of normality and adjustment for multiple comparisons
- A full description of the statistical parameters including central tendency (e.g. means) or other basic estimates (e.g. regression coefficient) AND variation (e.g. standard deviation) or associated estimates of uncertainty (e.g. confidence intervals)
- For null hypothesis testing, the test statistic (e.g. F , t , r) with confidence intervals, effect sizes, degrees of freedom and P value noted
Give P values as exact values whenever suitable.
- For Bayesian analysis, information on the choice of priors and Markov chain Monte Carlo settings
- For hierarchical and complex designs, identification of the appropriate level for tests and full reporting of outcomes
- Estimates of effect sizes (e.g. Cohen's d , Pearson's r), indicating how they were calculated

Our web collection on [statistics for biologists](#) contains articles on many of the points above.

Software and code

Policy information about [availability of computer code](#)

Data collection

We did not use software to collect data in this study.

Data analysis

We used IDseq v3.2 for mNGS data analysis (<https://github.com/chanzuckerberg/idseq-web>). We used Tableau Desktop 2018 for supplemental figures 4 and 5. We used GraphPad Prism 8 for violin plots in figures 1 and 3 and for supplemental figures 2, 3, 6, and 8. We used PEAR v0.9.8, bowtie2 v2.3.1, Python/Pandas v2.7.1, R studio 1.1.423 to analyze VirScan data as described before and cited in the manuscript (O'Donovan, B., et al. Exploration of Anti-Yo and Anti-Hu paraneoplastic neurological disorders by PhIP-Seq reveals a highly restricted pattern of antibody epitopes. in bioRxiv (2018)) and in the Methods. We used BLASTp 2.9.0 to map peptides to a reference enterovirus A71 sequence. We used Morpheus Heatmap (<https://software.broadinstitute.org/morpheus/>) to generate the heatmap in figure 1.

For manuscripts utilizing custom algorithms or software that are central to the research but not yet described in published literature, software must be made available to editors/reviewers. We strongly encourage code deposition in a community repository (e.g. GitHub). See the Nature Research [guidelines for submitting code & software](#) for further information.

Data

Policy information about [availability of data](#)

All manuscripts must include a [data availability statement](#). This statement should provide the following information, where applicable:

- Accession codes, unique identifiers, or web links for publicly available datasets
- A list of figures that have associated raw data
- A description of any restrictions on data availability

The non-human sequence reads from each sample were deposited at the National Center for Biotechnology Information Sequence Read Archive (PRJNA557094). The phage display data are provided both in the Supplemental Tables and as Extended Data in the manuscript.

Field-specific reporting

Please select the one below that is the best fit for your research. If you are not sure, read the appropriate sections before making your selection.

Life sciences Behavioural & social sciences Ecological, evolutionary & environmental sciences

For a reference copy of the document with all sections, see [nature.com/documents/nr-reporting-summary-flat.pdf](https://www.nature.com/documents/nr-reporting-summary-flat.pdf)

Life sciences study design

All studies must disclose on these points even when the disclosure is negative.

Sample size	We did not perform a power calculation. We analyzed as many CSF samples as we had access to.
Data exclusions	Residual banked CSF was obtained from children with other neurologic diseases (ONDs) without suspected primary EV infection and without known exposure to intravenous gamma globulin for controls.
Replication	We used n = 42 AFM cases and n = 58 OND controls. We replicated a subset of AFM cases and OND controls on VirScan and ELISA. We present data typical of the replicates.
Randomization	Samples were not randomized.
Blinding	Experimenters were not blinded.

Reporting for specific materials, systems and methods

We require information from authors about some types of materials, experimental systems and methods used in many studies. Here, indicate whether each material, system or method listed is relevant to your study. If you are not sure if a list item applies to your research, read the appropriate section before selecting a response.

Materials & experimental systems

Methods

n/a	Involvement in the study
<input type="checkbox"/>	<input checked="" type="checkbox"/> Antibodies
<input type="checkbox"/>	<input checked="" type="checkbox"/> Eukaryotic cell lines
<input checked="" type="checkbox"/>	<input type="checkbox"/> Palaeontology
<input checked="" type="checkbox"/>	<input type="checkbox"/> Animals and other organisms
<input type="checkbox"/>	<input checked="" type="checkbox"/> Human research participants
<input type="checkbox"/>	<input checked="" type="checkbox"/> Clinical data

n/a	Involvement in the study
<input checked="" type="checkbox"/>	<input type="checkbox"/> ChIP-seq
<input checked="" type="checkbox"/>	<input type="checkbox"/> Flow cytometry
<input checked="" type="checkbox"/>	<input type="checkbox"/> MRI-based neuroimaging

Antibodies

Antibodies used	HIS.H8 (MA1-21315, ThermoFisher Scientific), Goat anti-Human IgG (H+L), HRP (Invitrogen, A18805), Alkaline phosphatase secondary antibody (31320, ThermoFisher Scientific).
Validation	HIS.H8 is validated for Western Blot according to the manufacturer. Goat anti-Human IgG (H+L) HRP (A18805) is validated for ELISA according to the manufacturer. Alkaline phosphatase secondary antibody (31320) is validated for Western Blot according to the manufacturer.

Eukaryotic cell lines

Policy information about [cell lines](#)

Cell line source(s)	ExpiCHO cells (Thermo Fisher)
Authentication	The cell line was not authenticated.
Mycoplasma contamination	The cell line was not tested for mycoplasma contamination.
Commonly misidentified lines (See ICLAC register)	The cell line is not listed in the ICLAC database.

Human research participants

Policy information about [studies involving human research participants](#)

Population characteristics	<p>All patients were evaluated by board-certified neurologists at their respective enrollment sites, and some samples were obtained through the Centers for Disease Control and Prevention (CDC) or the California Department of Public Health (CDPH). Patients 1 through 8 were enrolled at Boston Children’s Hospital. Patients 25 through 28, and 47 through 100 were enrolled in a research study at UCSF (IRB number 13-12236) for pathogen and autoantibody detection for patients with idiopathic neuroinflammation. Patients 9 through 17 were enrolled through the University of Colorado (IRB number 12-0745). Patients 18 through 24 were from the CDPH. Patients 29-46 were from the Division of Viral Diseases at the CDC, with this work constituting public health surveillance as determined by the human subjects coordinator of the National Center for Immunization and Respiratory Disease. Electronic and paper medical records of patients from Boston Children’s Hospital, UCSF, the University of Colorado, and the CDPH were reviewed for demographic details, clinical data, laboratory results, and outcome at last follow-up.</p> <p>Age and sex were shared in aggregate from the CDC. Patient demographics are described in Table 1 with detailed information on available clinical diagnostic testing in Supplemental Tables S1A and S1B. The AFM cases were younger (median age 37.8 months, interquartile range [IQR], 11 to 64 months) than the OND controls (median age 120 months, IQR, 66 to 174 months), with a p-value of 0.0497 (as determined by an unpaired parametric t-test). There was a higher proportion of males in the AFM cases. AFM cases and OND controls from the Western and Northeastern USA (Supplemental Figure 2) make up the majority of both categories. Cases from 2018 make up the majority of the AFM cases.</p>
Recruitment	<p>AFM cases were recruited by participating sites if they met the inclusion criteria for patients with a confirmed diagnosis of definite or probable acute flaccid myelitis as outlined by the Council of State and Territorial Epidemiologists (Supplemental Table 1). OND controls were recruited as part of an ongoing research study investigating the etiologies of neuroinflammatory diseases.</p>
Ethics oversight	<p>UCSF (IRB number 13-12236), University of Colorado (IRB number 12-0745), California Department of Public Health (CDPH), Division of Viral Diseases at the CDC, with this work constituting public health surveillance as determined by the human subjects coordinator of the National Center for Immunization and Respiratory Disease.</p>

Note that full information on the approval of the study protocol must also be provided in the manuscript.

Clinical data

Policy information about [clinical studies](#)

All manuscripts should comply with the ICMJE [guidelines for publication of clinical research](#) and a completed [CONSORT checklist](#) must be included with all submissions.

Clinical trial registration	This study was not a clinical trial.
Study protocol	This study was not a clinical trial.
Data collection	This study was not a clinical trial.
Outcomes	This study was not a clinical trial.